A

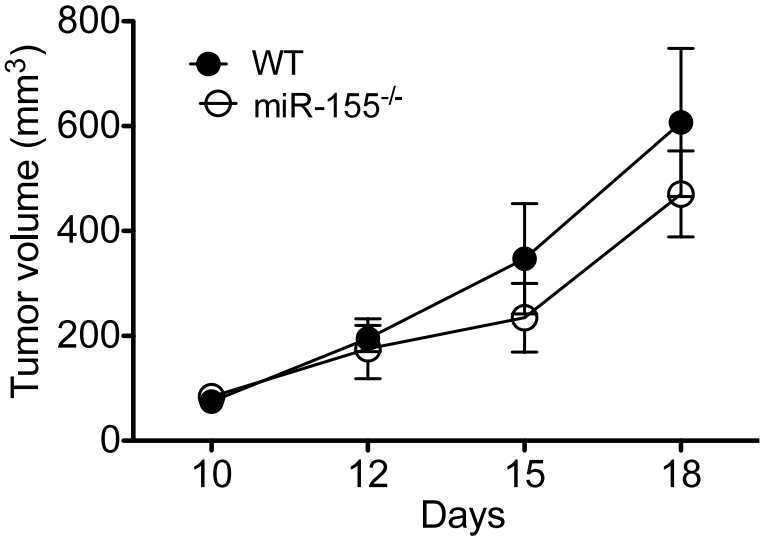

B

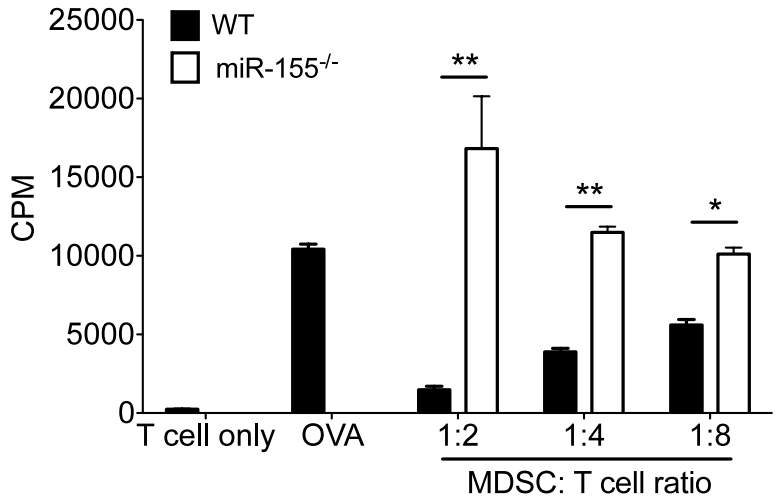

Supple. Fig. 1

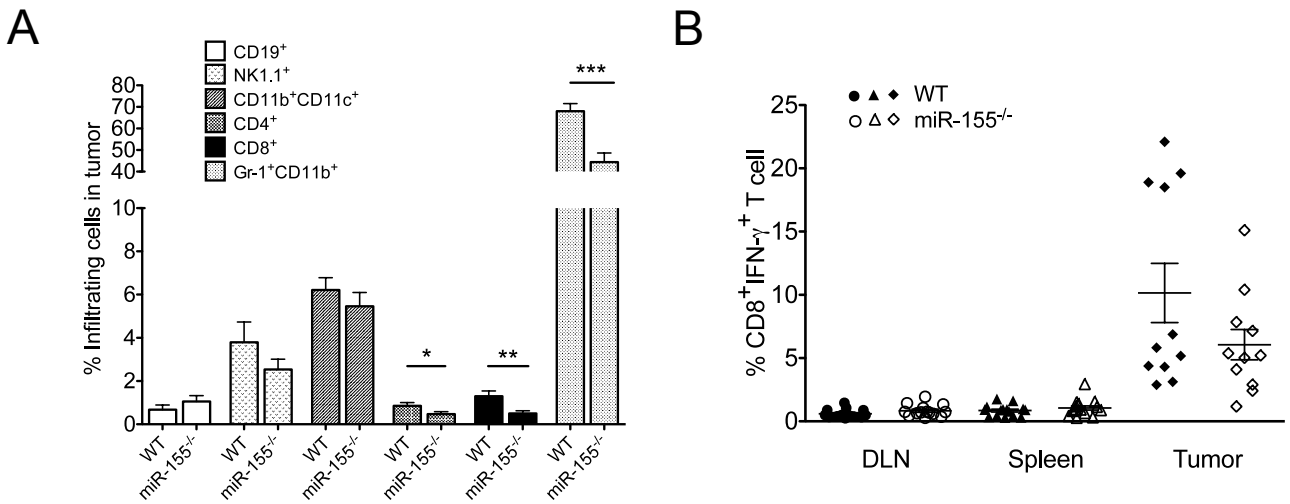
A
CD19+
NK1.1+
CD11b+CD11c+
CD4+
CD8+
Gr-1+CD11b+
% Infiltrating cells in tumor
WT
miR-155-/-
*
**
***
B
WT
miR-155-/-
% CD8+IFN-γ+ T cell
DLN
Spleen
Tumor

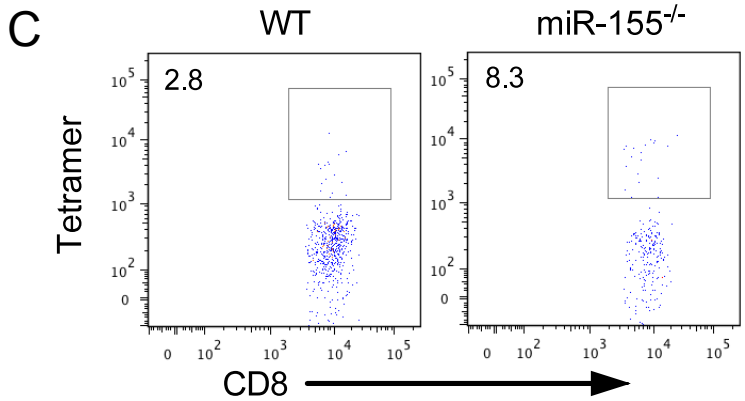
C
WT
miR-155-/-
2.8
8.3
Tetramer
CD8

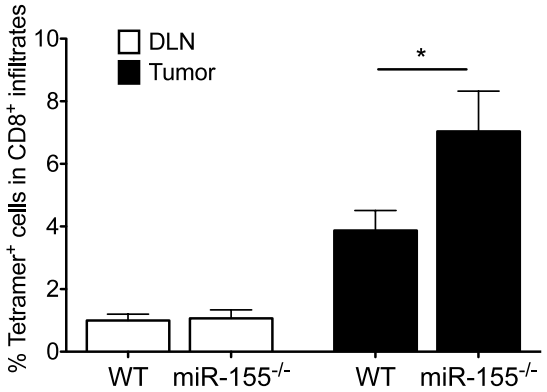
DLN
Tumor
*
% Tetramer+ cells in CD8+ infiltrates
WT
miR-155-/-
WT
miR-155-/-

Supple. Fig. 2

A

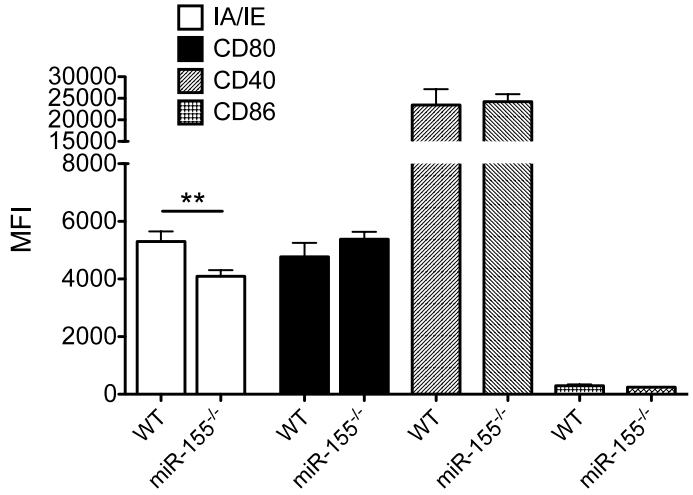

B

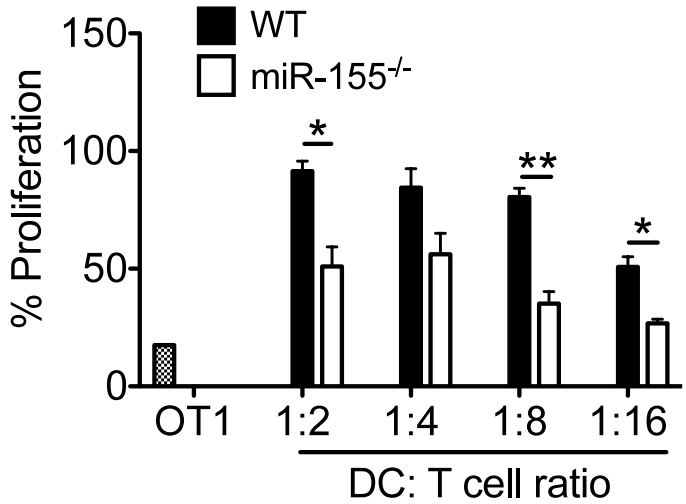

C

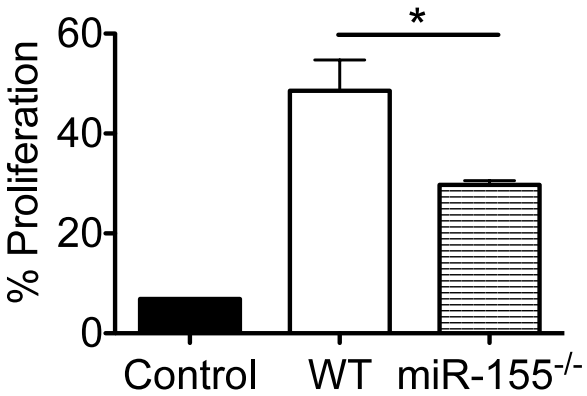

Supple. Fig. 3

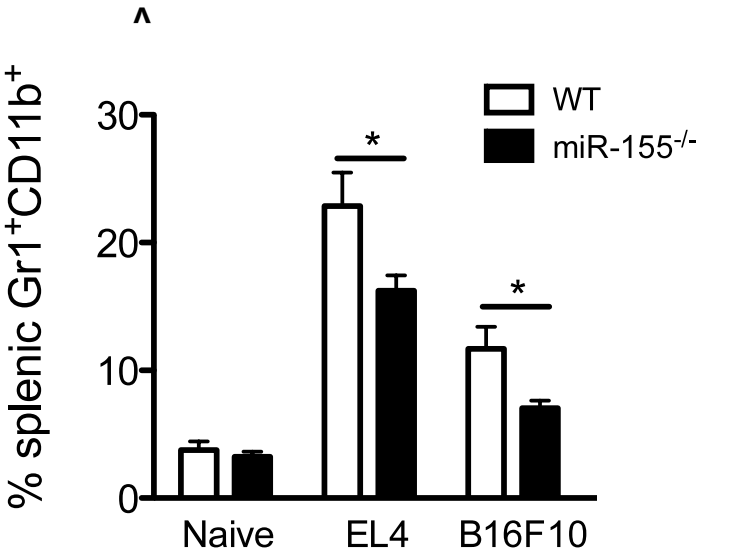
^
% splenic Gr1+CD11b+
30
20
10
0
WT
miR-155-/-
*
*
Naive
EL4
B16F10

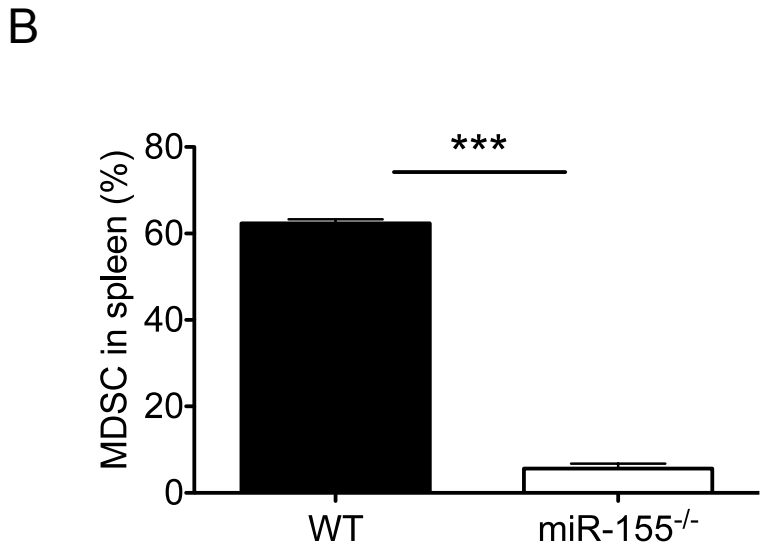
B
MDSC in spleen (%)
80
60
40
20
0
***
WT
miR-155-/-

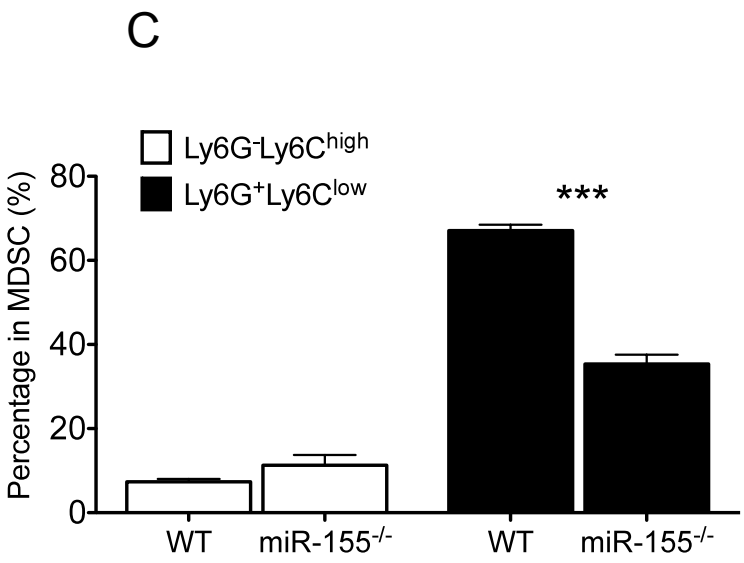
C
Ly6G-Ly6Chigh
Ly6G+Ly6Clow
Percentage in MDSC (%)
80
60
40
20
0
***
WT
miR-155-/-
WT
miR-155-/-

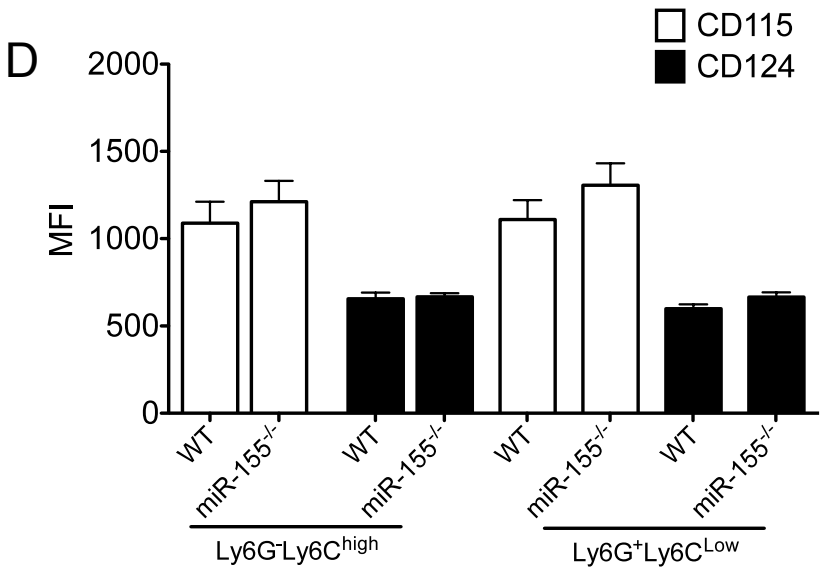
D
CD115
CD124
MFI
2000
1500
1000
500
0
WT
miR-155-/-
WT
miR-155-/-
WT
miR-155-/-
WT
miR-155-/-
Ly6G-Ly6Chigh
Ly6G+Ly6CLow

Supple. Fig. 4

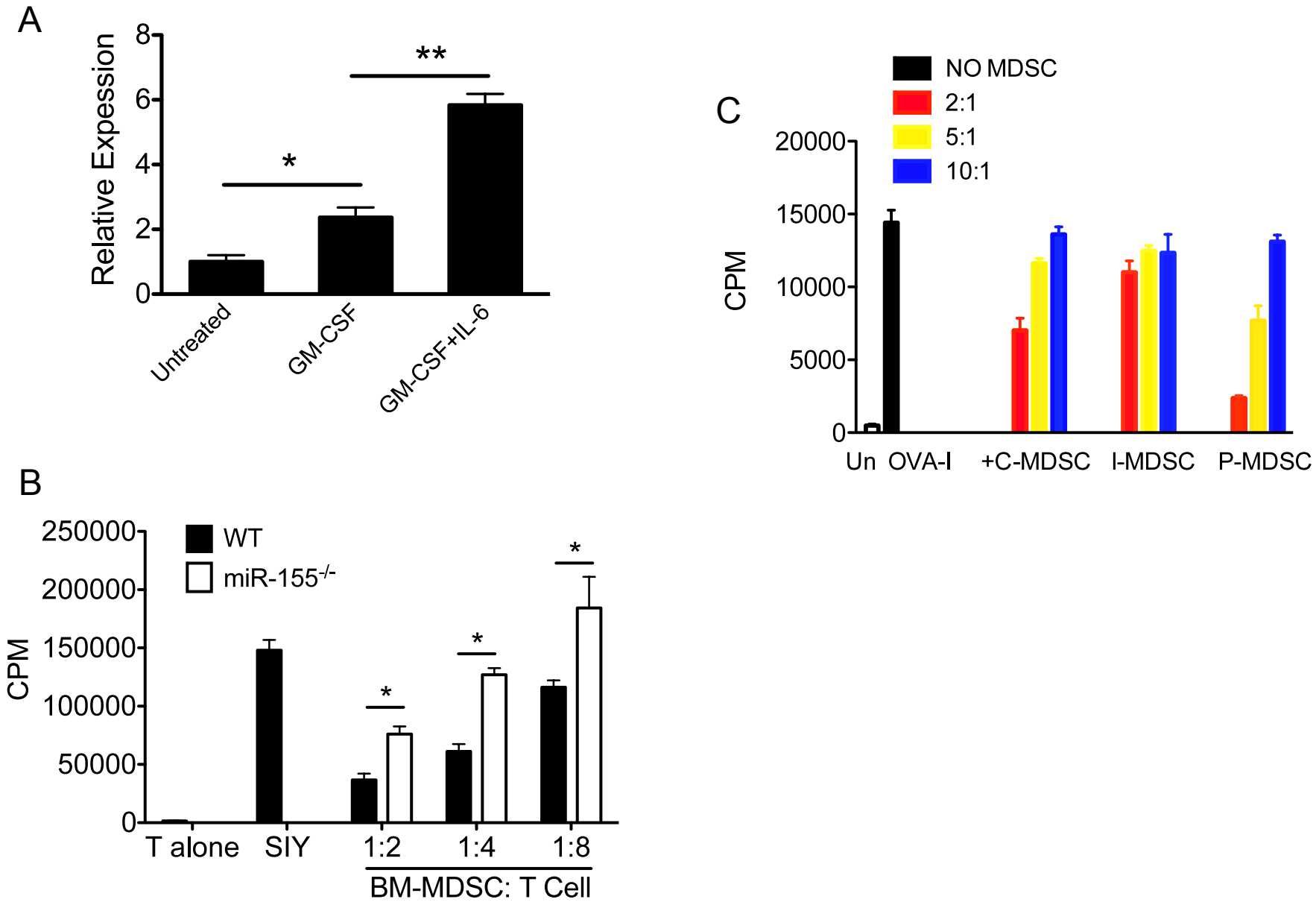
A
Relative Expression
8
6
4
2
0
**
*
Untreated
GM-CSF
GM-CSF+IL-6
B
CPM
250000
200000
150000
100000
50000
0
WT
miR-155-/-
*
*
*
T alone
SIY
1:2
1:4
1:8
BM-MDSC: T Cell
C
NO MDSC
2:1
5:1
10:1
CPM
20000
15000
10000
5000
0
Un
OVA-I
+C-MDSC
I-MDSC
P-MDSC

Supple. Fig. 5

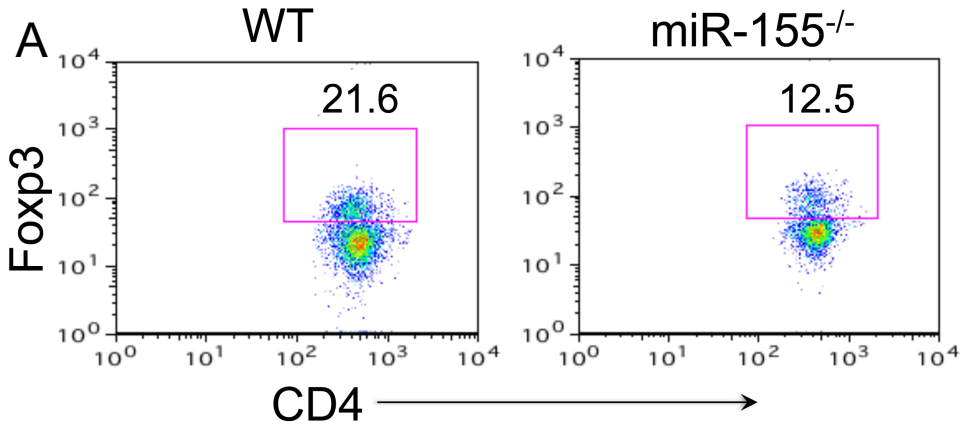
A
WT
miR-155-/-
21.6
12.5
Foxp3
CD4

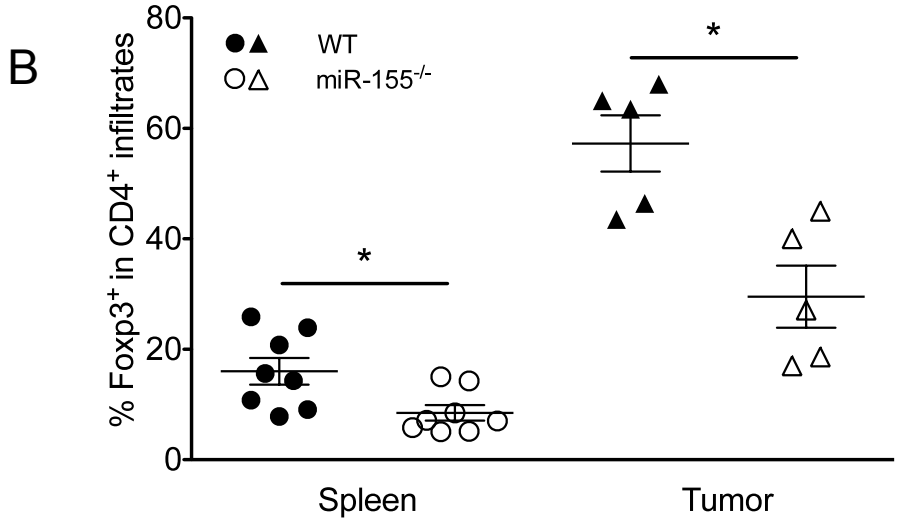
B
WT
miR-155-/-
% Foxp3+ in CD4+ infiltrates
80
60
40
20
0
*
*
Spleen
Tumor

Supple. Fig. 6

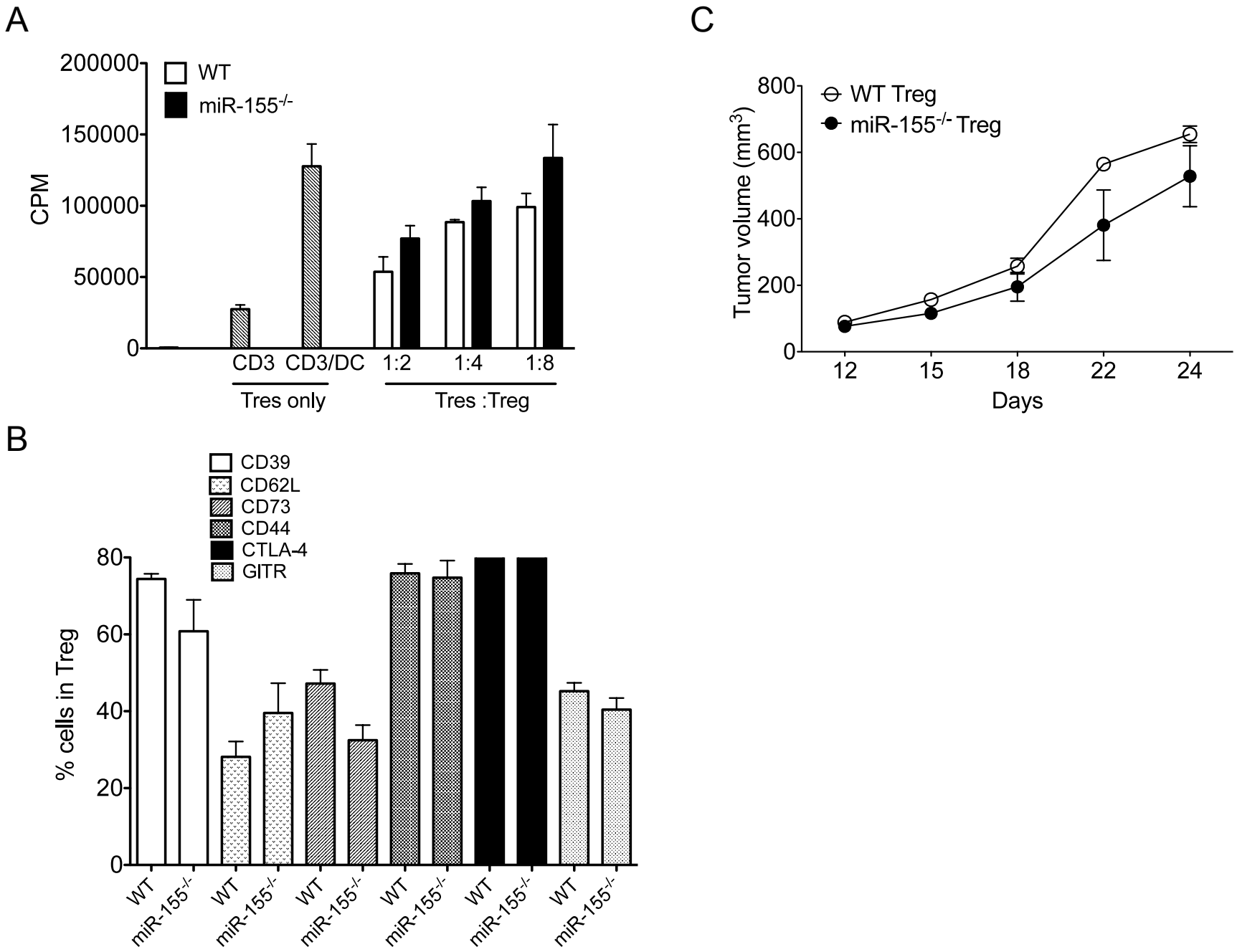
A
200000
150000
100000
50000
0
CPM
WT
miR-155-/-
CD3
CD3/DC
1:2
1:4
1:8
Tres only
Tres :Treg
B
CD39
CD62L
CD73
CD44
CTLA-4
GITR
80
60
40
20
0
% cells in Treg
WT
miR-155-/-
C
800
600
400
200
0
Tumor volume (mm3)
WT Treg
miR-155-/- Treg
12
15
18
22
24
Days

Supple. Fig. 7

Supplemental Figure 1. Tumor growth in miR-155-deficient mice. WT or miR-155$^{-/-}$ mice (n=5) were inoculated s.c. with 10^6 B16-SIY cells (**A**). Tumor volume was measured every 3 days. (**B**) The suppressive activity of MDSCs sorted from B16-SIY-bearing WT or miR-155$^{-/-}$ mice. Sorted WT or miR-155$^{-/-}$ tumor-infiltrating Gr1$^+$CD11b$^+$ MDSCs were added at different ratios to OT-I splenocytes stimulated with OVA-I peptides for 3d, and 3[H] thymidine uptake was measured. *, p<0.05; **, p<0.01.

Supplemental Figure 2. Host miR-155 deficiency enhanced antigen-specific antitumor T cell immunity. (**A**) Percent CD4$^+$, CD8$^+$, Gr1$^+$CD11b$^+$, CD45$^+$CD19$^+$ and CD49b$^+$NK1.1$^+$ cells in tumor infiltrates of WT or miR-155$^{-/-}$ mice collected 14-21 days after inoculation with LLC1-OVA tumor cells (n=10-19). (**B**) CD8$^+$IFN-γ$^+$ T cell frequency in spleen, DLN and tumor from LLC1-OVA-bearing WT or miR-155-/- mice 14-21 days after tumor inoculation (n=11-15). (**C**) Representative flow analysis of tumor antigen-specific CD8$^+$ T cell tumor infiltrates from LLC1-OVA-bearing WT or miR-155$^{-/-}$ mice. Frequency of tetramer$^+$ cells specific for the OVA epitope SIINFEKL in CD8$^+$ infiltrates from mice in **B**, was summarized (n = 5). *, p<0.05; **, p<0.01; ***, p<0.001.

Supplemental Figure 3. miR-155 is required for optimal function of DCs and T cells from tumor-bearing mice. (**A**) Flow analysis for cell surface expression of IA/IE, CD80, CD40 and CD86 on tumor-infiltrating myeloid DC (CD11b$^+$CD11c$^+$) from LLC1-OVA tumor-bearing mice. The results are

summarized from three repeated experiments. (**B**) Sorted tumor-infiltrating DCs from WT or miR-155$^{-/-}$ tumor-bearing mice were added at different ratios to stimulate CFSE-labeled OT-I CD8^{+} T cells for 3d. The dilution of CFSE was detected by flow cytometry and the results were summarized. (**C**) Sorted tumor-infiltrating CD8^{+} T cells from WT or miR-155$^{-/-}$ tumor-bearing mice were labeled with eFluor450 and added at 1:2 to WT DCs stimulated with OVA-I peptides for 3d. The dilution of eFluor450 was detected by flow cytometry and the results were summarized. *, $p<0.05$; **, $p<0.01$.

Supplemental Figure 4. miR-155 is required for splenic MDSC accumulation in different tumor models. (**A**) Percentages of splenic Gr1^{+}CD11b^{+} MDSCs were determined by flow cytometry from EL4-, B16F10- and (**B**) LLC1 tumor-bearing mice (n=5). *, $p<0.05$. (**C**) Percentages of splenic CD11b^{+}Ly6G^{+}Ly6C^{low} (granulocytic) and CD11b^{+}Ly6G^{-}Ly6C^{high} (monocytic) MDSCs from WT or miR-155$^{-/-}$ LLC1 tumor-bearing mice were determined by flow cytometry. (**D**) Expression of CD115 and CD124 on both MDSC subsets above was determined by flow cytometry. The MFI (mean fluorescence intensity) of CD115 or CD124 expression was summarized (n = 5).

Supplemental Figure 5. miR-155 regulates BM-derived MDSC. (**A**) BM cells were cultured with GM-CSF or GM-CSF+IL-6 for 3 d and miR-155 expression was assayed by quantitative real-time PCR (n=3). (**B**) The suppressive activity of the GM-CSF and IL-6-conditioned BM-derived MDSCs from miR-155$^{-/-}$ mice

versus WT mice. (**C**) The suppressive activity of the GM-CSF and IL-6-conditioned BM-derived MDSCs by the transfection with pre-miR-155/BIC (P-MDSC), miR-155 inhibitor miRNA (I-MDSC) or control oligonucleotides (C-MDSC) by AMAXA. *, $p<0.05$.

Supplemental Figure 6. Decreased accumulation of Tregs in miR-155-deficient tumor-bearing mice. (**A**) Representative dot plots of Foxp3 expression in EG7 tumor-infiltrating $CD4^+$ cells. (**B**) Percent $Foxp3^+$ cells among $CD4^+$ cells from spleen and tumor tissues of EG7-bearing WT or miR-$155^{-/-}$ mice were summarized (n=5). *, $p<0.05$; **, $p<0.01$.

Supplemental Figure 7. Suppressive activity and tumor-promoting role of miR-155-deficient Tregs. (**A**) WT or miR-$155^{-/-}$ $CD4^+CD25^+$ Tregs were sorted and added at different ratios to CFSE-labeled $CD4^+CD25^-$ Tres cells stimulated with anti-CD3 and WT DCs for 3d. The dilution of CFSE was detected by flow cytometry and the results were summarized. (**B**) Percentages of CD39, CD73, GITR, CD44, CD62L and CTLA4 expression among splenic $CD4^+CD25^+Foxp3^+$ Tregs from WT or miR-$155^{-/-}$ LLC1-bearing mice were measured by flow cytometry. (**C**) Sorted WT or miR-$155^{-/-}$ splenic $CD4^+CD25^+$ Tregs were injected i.v. into LLC1-bearing mice on d7, d14 and d20. Tumor volumes were measured every 3 days.